Journal of Science and Technology
ISSN: 2456-5660 Volume 7, Issue 02 (MAR-APR 2022)

www.jst.org.in *DOI: https://doi.org/10.46243/jst.2022.v7.i02.pp54-76*

Ligands tris(2-pyridylmethyl)amine with nitrile group in α-substituted and the corresponding $FeCl_2$ complexes: a diversity preceding a possible using of dioxygen in soft conditions

Dr. Nasser Thallaj: *Faculty of Pharmacy. Al Rasheed Private University. Damascus, Syria*

To Cite this Article
*Dr. Nasser Thallaj, "***Ligands tris(2-pyridylmethyl)amine with nitrile group in α-substituted and the corresponding $FeCl_2$ complexes: a diversity preceding a possible using of dioxygen in soft conditions***", Journal of Science and Technology, Vol. 07, Issue 02, March-April 2022.*

Article Info
Received: 14-02-2022 *Revised: 28-02-2022* *Accepted:08-03-2022* *Published: 15-03-2022*

Abstract

We have synthesized the mono, bis and tris nitrile at the α position ligands in the tris(2-pyridylmethyl)amine (TPA) series, respectively CNTPA, (CN)2TPA and (CN)3TPA. Nitrile at the α position of these nitrogen-containing tripods shifts the oxidation potential of the ligand by comparison with the TPA ligand, it is observed that the oxidation potentials of the ligands increase regularly with the number of nitrile groups. For each group added, the oxidation potential is increased by an average of 110mV / ECS. This reflects the strong electron-withdrawing effect of the nitrile groups.. The crystal structure analysis of the dichloroferrous complexes with CNTPA and (CN)2TPA reveals that the iron lies in a distorted octahedral geometry comparable to that already found in $TPAFeCl_2$. All spectroscopic data indicate that the geometry is retained in solution. These three isostructural complexes all react with molecular dioxygen to yield µ-oxo diferric complexes as stable compounds. Upon reduction, all µ-oxo diferric complexes convert back into the starting ferrous species. The oxygenation reaction parallels the well known formation of µ-oxo derivatives from dioxygen in chemistry of porphyrins reported almost three decades ago. The crystal structure analysis is reported for each of these three µ-oxo compounds. With TPA, a symmetrical structure is obtained for a dicationic compound, the tripod coordinating in the (κ^4-N) coordination mode. With CNTPA, the compound is a neutral µ-oxo di-ferric complex. When oxygenation is carried out on the (CN)2TPA complex, a neutral asymmetrical compound is obtained. The striking point within the series of ferrous precursors is the effect of the ligand on the kinetics of oxygenation of the complexes. Whereas the parent complex undergo full oxygenation over 14 hours, the mono ***nitrile*** ligand provides a complex that has fully reacted over 14 hours, the reaction time being only 2 hours for the complex with the dinitriles ligand,and for trinitriles ligand it will tack 30min. Thus electron-deficiency (Lewis acidity at the metal centre) seems to govern the kinetics of oxygenation. This strongly suggests coordination of the dioxygen as an initial step in the process leading to formation of µ-oxo diferric compounds, by contrast with un unlikely outer sphere reduction of dioxygen, that generally occurs at very negative potentials. Finally, we report that cyclohexane is catalytically converted into cyclohexanone when reacted with dioxygen in the presence of zinc amalgam, and that the conversion rate also parallels the Lewis acidity at the metal center, with the best rate obtained for with $(CN)2TPAFeCl_2$.

www.jst.org.in *DOI: https://doi.org/10.46243/jst.2022.v7.i02.pp54-76*

Kye words: Complexes of iron$^{(II)}$ with ligands CNTPA, (CN)2TPA and (CN)3TPA in α-substituted, Biomimetic Molecular dioxygen activation, tris(2-pyridylmethyl)amine.

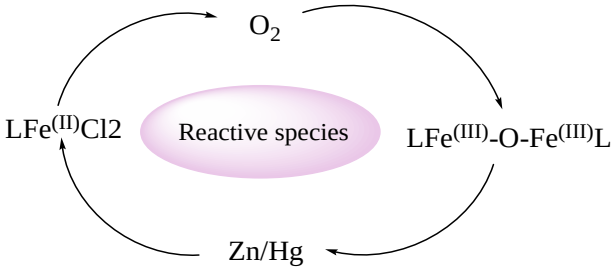

Introduction:

The catalysis of oxygen transfer to organic substrates is well known in biology and can be carried out by enzymes containing metalloproteins possessing an iron center of the heme type (cytochromes P-450 for example) or non-heme (methane monooxygenase by example) [1]. These reactions can be carried out using molecular oxygen. In this case, it must be fixed. Then there can either be formation of a hydroperoxo-reactive species or cleavage of the O-O bond. In the latter case, highly reactive metal – oxo compounds are formed [2]. Iron complexes with tris (2-pyridyl methyl) amine (TPA) tetradente ligands and some of its derivatives have been well studied over the past ten years . Some of them show functional analogies with certain non-heme iron enzymes involved in the activation of oxygen [3]. However, in the majority of cases, hydroperoxides are used as oxygen donating agents [4-7]. Molecular oxygen has been well used, however, but it only reacts with ferrous compounds which are already coordinated with substrates which activate the metal, such as catechols or thiolates for example [8-10]. Another well studied enzyme in biological systems is tryptophan hydroxylase, which catalyzes a key step in serotonin biosynthesis and plays important roles in the circadian rhythms [11-17]. The study of a series of dichloroferrous complexes with substituted TPA-type ligands was undertaken in the laboratory [18-19]. On the ligand, the -substitution of nitrogen can induce trident coordination of the ligand (potentially tetradent). The complexes thus formed can react with molecular oxygen without particular activation, provided that the ligand is substituted by halogens. There is therefore here a double effect, steric and electronic. One of our goals of is to build artificial systems that are active with respect to molecular oxygen. Ideally, this requires the presence of an oxygen binding site, an electron source (external or grafted) and a site protection matrix, the latter of the protein type, or why not inorganic (zeolite, electrod) or organic (dandrmere,or nanomaterials, for example). In any case, it is important to be able to have a set of functional complexes which also have an interesting reactivity. This is the context in which this study is situated. First, we prepared ligands of TPA structure mono, bi, and tri-substituted by ***nitrile*** functional groups. Their synthesis will be described. We will then present the coordination chemistry of these ligands, which we approach by the preparation of dichloroferrous complexes. One of the complexes prepared has been completely

characterized and studied in solution. Finally, we will describe the first studies of the reactivity of this complex with respect to molecular oxygen.

Matrials and methods

Preparation 2-nitrile-6-methylpyridine:

A solution of 24.6 g (0.200 mol) of 2-methylpyridine-1-oxide in 200 cm3 of dichloromethane is dried over magnesium sulfate. This solution is transferred by cannula into a flask containing 25.0 g (0.253 mol) of trimethylsilyl cyanide. 21.4g (0.253 mol) of dimethylcarbamyl chloride are dissolved in 50 cm3 of dichloromethane and this solution is added gradually (30 minutes) to the previous mixture using a dropping funnel. The reaction mixture is kept under stirring for 24 hours. 200 cm3 of a 10% aqueous solution of potassium carbonate are then added gradually. The product is extracted several times with dichloromethane and the combined phases dried over magnesium sulfate. The solvent is evaporated off and after recrystallization from pentane, 26.0 g (0.220 mol) of a white solid are obtained. The yield is 98%.

RMN ^1H *, δ, ppm, CDCl*$_3$: 7.70(t,1H,CH_γ); 7.50(d,1H,$CH_{\beta'}$); 7.37(d,1H,CH_β); 2.60(s,3H,CH_3).

Preparation 2-nitrile-6-bromomethylpyridine:

In a flask containing 10.0g (0.084 mol) of 2-nitrile-6-methylpyridine in 200 cm3 of carbon tetrachloride, are added 16.6g (0.093 mol) of N-bromosuccinimide and 0.2g (0.840 mol) of benzoïl peroxide. The reaction mixture, with stirring, is heated at reflux (90 ° C.) for 6 hours. The solid residues are filtered off and the solvent is evaporated. The product is then dissolved in dichloromethane and poured onto a silica column (Ø = 4 cm) mounted in toluene. This solvent is used as an eluent, and makes it possible to obtain 4 fractions. Fraction 3 containing the product is evaporated, 3.0g (0.015 mol) of a pale yellow solid are obtained. The yield is 18%.
RMN ^1H*, δ, ppm, CDCl*$_3$: 7.86(t,1H,CH_γ); 7.69(dd,1H,$CH_{\beta'}$); 7.62(dd,1H,CH_β); 4.55(s,2H,CH_2).

TPACN preparation:

In a flask containing 1.00g (5.07 mmol) of 2-nitrile-6-bromomethylpyridine in 100 cm3 of acetonitrile, are added 1.01g (5.07 mmol) of dimethylpyridineamine and 0.54g (5.07 mmol) of sodium carbonate. The reaction mixture, with stirring, is heated at reflux (95 ° C.) for 18 hours. The solid residues are filtered and then the solvent is evaporated off. The product is then taken up in a dichloromethane / water mixture and extracted several times with dichloromethane. The combined phases are dried over magnesium sulfate. The solvent is evaporated off and after recrystallization from pentane, 1.29 g (4.11 mmol) of a white solid are obtained. The yield is 81%.
Elemental analysis:C% =72.63 H%=5.08 N%=22.42
(theoretical values.: C% =72.36 H%=5.43 N%=22.21)
RMN ^1H*, δ, ppm, CDCl*$_3$: 8.53(m,2H,CH_α); 7.82(dd,1H,$CH_{\beta1}$); 7.77(t,1H,$CH_{\gamma1}$); 7.65 (td,2H,CH_γ); 7.54(dd,1H,$CH_{\beta1'}$); 7.51(dt,2H,$CH_{\beta'}$); 7.15(m,2H,CH_β); 3.92 (s,2H,CH_2); 3.88 (s,4H,CH_2).
RMN^{13}C **:** 162(1C,2') ; 159(2C,2) ; 149(2C,6) ; 137(1C,4') ; 136(1C,4) ; 132(1C,6') ; 127(1C,3') ; 126(1C,5') ; 123(2C,3) ; 122(2C,5) ; 117(1C,CN) ; 60(2C,CH_2) ; 59(1C,CH_2).
I.R.: $\nu_{(CN)}$=2539 cm^{-1}.

TPACN2 preparation:

In a flask containing 1.40g (7.10 mmol) of 2-nitrile-6-bromomethylpyridine in 100 cm3 of acetonitrile, are added 0.40g (3.55 mmol) of pycolylamine and 0.37g (3.55 mmol) of sodium carbonate. The reaction mixture, with stirring, is heated at reflux (95 ° C.) for 18 hours. The solid residues are filtered and then the solvent is evaporated off. The product is then taken up in a dichloromethane / water mixture and extracted several times with dichloromethane. The combined phases are dried over magnesium sulfate. The solvent is evaporated off and after recrystallization from pentane, 1.17 g (3.44 mmol) of a white solid are obtained. The yield is 97%.
Elemental analysis:C%=70.18 H%=4.79 N%=24.23
(theoretical values.:: C%=70.57 H%=4.74 N%=24.69)
RMN ^1H*, δ, ppm, CDCl*$_3$: 8.545(m, 1H,CH_α); 7.802(dd,2H,$CH_{\beta1}$); 7.794(dd,2H,$CH_{\beta1'}$); 7.665(td,1H,CHγ); 7.566(dd,2H,$CH\gamma_1$), 7.473(dt,1H,$CH_{\beta'}$); 7.169(m,1H,CH_β); 3.993(s,4H,CH_2); 3.889(s,2H,CH_2).
RMN ^{13}C : 161(2C,2'); 158(1C,2); 149(1C,6); 137(2C,4'); 136(1C,4); 133(2C,6'); 127(2C,3'); 126(2C,5') ; 123(1C,3) ; 122(1C,5) ; 117(2C,CN) ; 60(1C,CH_2) ; 59(2C,CH_2).
IR :$\nu_{(CN)}$=2536 cm^{-1}.

TPACN3 preparation:

In a flask containing 3.00g (15.23 mmol) of 2-nitrile-6-bromomethylpyridine in 100 cm3 of tetrahydrofuran, are added 0.26g (4.08 mmol) of ammonium chloride and 0.20g (5.08 mmol) of sodium hydroxide. The flask is quickly sealed and the reaction mixture is kept under stirring for 3 days. The solid residues are filtered and then the solvent is evaporated off. The product is then taken up in a dichloromethane / water mixture and extracted several times with dichloromethane. The combined phases are dried over magnesium sulfate. The solution is concentrated and poured onto a silica column (Ø = 4 cm) mounted with dichloromethane. This solvent is used as an eluent to remove traces of starting material and then a 50% / 50% mixture of dichloromethane and acetone is used to recover the product. The solvent is evaporated off, 4.1 g (11.23 mmol) of a white solid are obtained. The yield is 74%.

Elemental analysis:C%=69.33 H%=4.298 N%=26.47
(theoretical values.:: C%=69.04 H%=4.11 N%=26.85)
RMN ^{1}H, δ, ppm, DMSO : 7.99(t,3H,$CH\gamma_1$); 7.88(d,3H,$CH_{\beta 1'}$); 7.85(d,3H,$CH_{\beta 1}$); 3.94(s,6H,CH_2)
RMN ^{13}C : 161(3C,2) ; 139(3C,4) ; 132(3C,6) ; 128(3C,3) ; 127(3C,5) ; 118(3C,CN) ; 60(3C,CH_2).
IR : $\nu_{(CN)}$=2538 cm^{-1}.

General method for complexation:

These reactions are carried out in the strict absence of O2, therefore under an argon atmosphere, and require the use of distilled and degassed solvents. 100 cm3 of tetrahydrofuran are transferred by cannula into a schlenck tube containing ferrous chloride (0.9 equivalent). This solution is in turn transferred by cannula to a second schlenck tube containing 0.2 g (1equivalent) of ligand. The reaction mixture which rapidly takes on a pinkish color is kept under stirring for 10 hours. The solvent is filtered through a cannula and a solid product is obtained after evaporation on a vacuum manifold. Then the complex is dissolved in acetonitrile, precipitated and then washed with ether. After filtering the ether, the complex is dried overnight on a vacuum ramp.

Resulets and discussion

General methodology implemented for the preparation of ligands of TPA structure.

We wish to obtain mono, bi or tri α-substituted compounds of TPA structure. This involves the preparation of the starting materials necessary to carry out the synthesis (Figure1) as described below. The preparation of the starting products substituted in the α- position is relatively easy usully but despite a particular difficulty encountered in the case of 2- ***nitrile*** -6-methylpyridine, due to the sensitivity of the reaction to the presence of water . Recrystallization of 2- ***nitrile*** -6-methylpyridine from pentane or hexane gives a yellowish-white crystalline product. We use the route involving the condensation of halomethyl pyridine derivatives. For most of them, these products are not commercial. It is therefore necessary to prepare them.

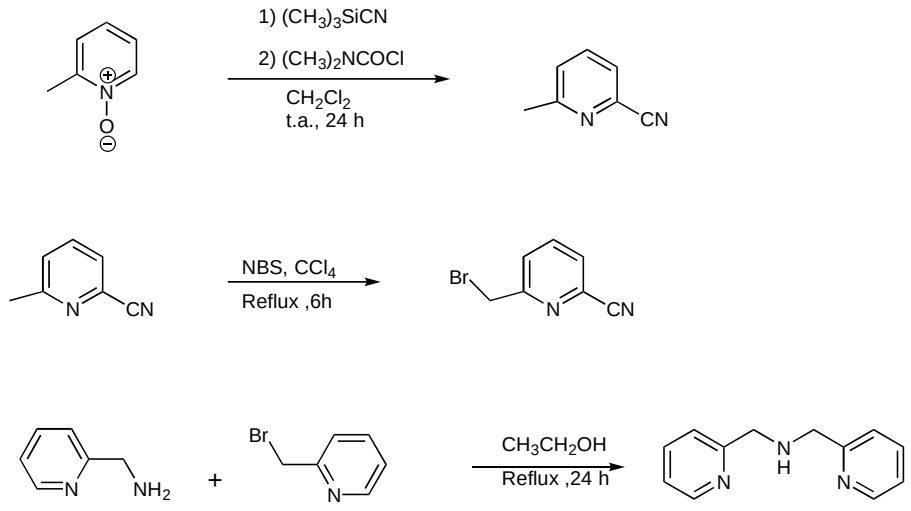

Figure 1: preparation of the starting materials necessary these products are not commercialy availale.

To make an aminomethylpyridine trident ligand, consists in reacting an aminomethylpyridine with a pyridine derivative having a halogenated benzyl position. For the preparation of DPA, it is necessary to work with a slight excess of amine, which can easily be removed by distillation The yields obtained are generally around 90% for the DPA.

1) Synthesis of CNTPA: According to the conventional method used in the laboratory, the synthesis of a mono-substituted tris (2-pyridylmethyl) amine (TPA) ligand is a second-order nucleophilic substitution reaction carried out from bis (2-pyridylmethyl) amine (DPA)) and the appropriate brominated reagent, here 6-nitrile-2-bromomethyl pyridine, in the presence of a base.

2) Synthesis of (CN)2TPA:The preparation of the (CN)2TPA ligand is carried out this time in the presence of two equivalents of 6-nitrile-2-bromomethyl pyridine derivative and one equivalent of amine, picolylamine.

3) Synthesis of (CN)3TPA:This involves reacting in a sealed bottle the 6-nitrile-2-bromomethyl pyridine derivative with ammonia generated in situ by the action of sodium hydroxide on ammonium chloride. It is a compound which is poorly soluble in common solvents.

www.jst.org.in *DOI: https://doi.org/10.46243/jst.2022.v7.i02.pp54-76*

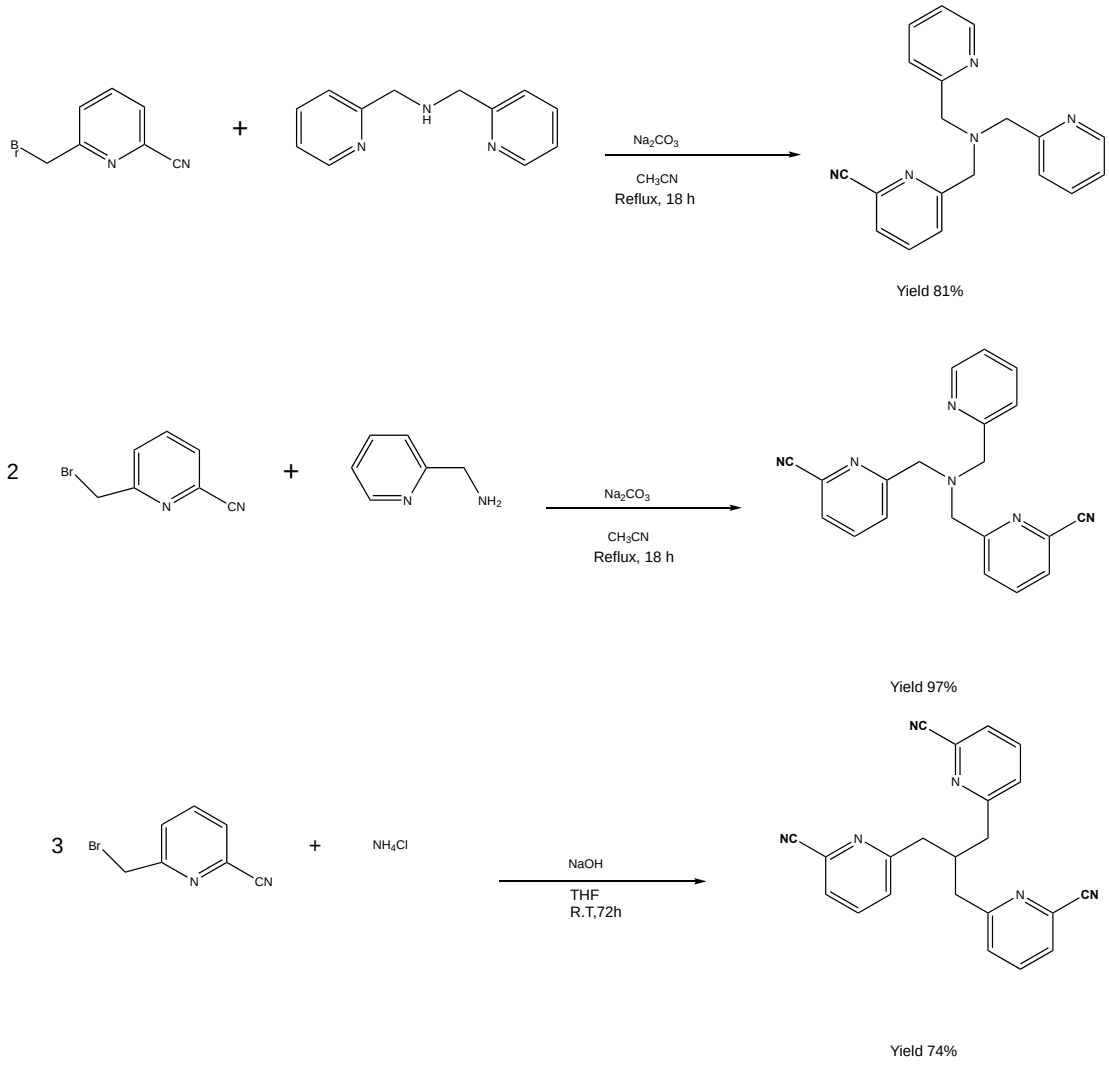

Figure 2: Preparation of (TPA) series respectively CNTPA, (CN)2TPA and (CN)3TPA.

After treatment, a white solid is obtained by recrystallization from pentane. The product was characterized by elemental analysis, 1H and 13C NMR, IR and cyclic voltammetry.

Comparison of the oxidation potentials of the ligands obtained

These measurements were carried out for the ligands CNTPA, (CN)2TPA and (CN)3TPA in solution in acetonitrile at room temperature. The value of TPA being already known, here are the results obtained (scanning speed: 200mV / s; support electrolyte: TBAPF6 0.1 M; platinum electrodes, ECS) Figure3.

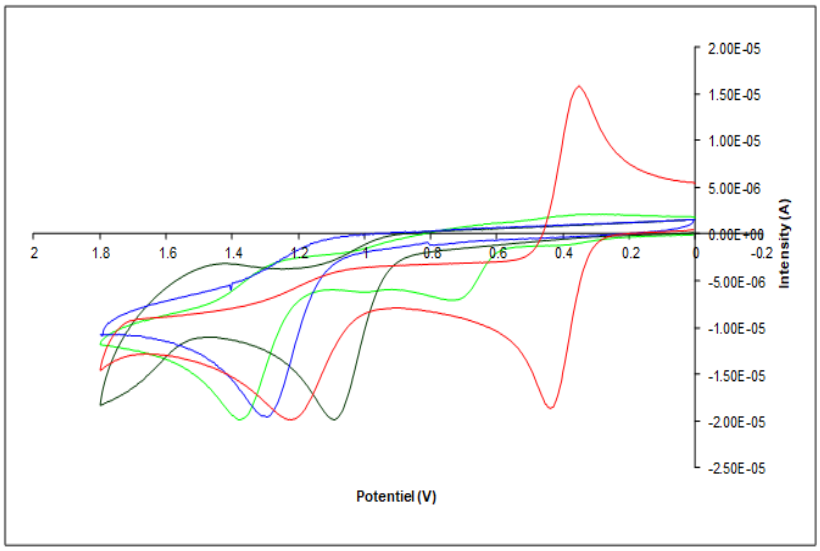

Figure3: Voltammerogram of ligands(TPA; CNTPA; (CN)2TPA;and (CN)3TPA), with TPA in black, CNTPA in red, (CN)2 TPAin blue, (CN)3TPAin green.

	TPA	**CNTPA**	**(CN)2TPA**	**(CN)3TPA**
E_a (V/ECS)	1.12	1.25	1.34	1.45

For each ligand, we get an irreversible wave corresponding to the oxidation of the central amine, the (CN)3TPA plot shows another less intense irreversible wave at Ea = 0.73 V / ECS whose origin we do not know. The reversible wave at E1 / 2 = 0.382 V / ECS corresponds to the redox potential of the ferrocene / ferrocenium pair used here as a reference (Figure 3). By comparison with the TPA ligand, it is observed that the oxidation potentials of the ligands increase regularly with the number of nitrile groups (the same effect having been observed for the fluorinated series). For each group added, the oxidation potential is increased by an average of 110mV / ECS. This reflects the strong electron-withdrawing effect of the nitrile groups.

The ligands CNTPA; (CN)2TPA and (CN)3TPA were metallated with anhydrous ferrous chloride FeCl2 (+ II). These reactions are carried out in the strict absence of O2, therefore under an argon atmosphere, and require the use of distilled and degassed solvent. In principle, a small excess of ligand (10%) is used for practical reasons of further processing.

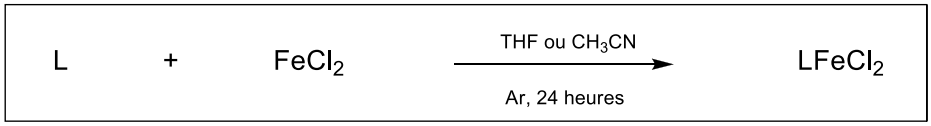

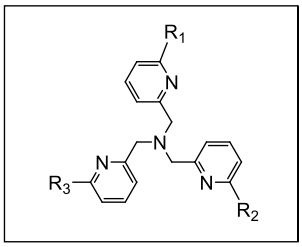

CNTPA: $R_1 = CN, R_2 = R_3 = H$
$(CN)_2$TPA: $R_1 = R_2 = CN, R_3 = H$
$(CN)_3$TPA: $R_1 = R_2 = R_3 = CN$

During the reaction, a reddish coloration of the solution is noticed for the three complexes. At the end of the reaction, the treatment involves evaporating the THF, taking it up with acetonitrile and precipitating the solid with ether. It is very probable that the reaction is quantitative but note that during the treatment more or less important quantities of compound are lost. The complexes are then characterized by paramagnetic 1H NMR, UV-visible, electrochemistry, conductimetry and if possible X-ray diffraction.

I. Characterization of the complexes by UV-visible spectroscopy.

The spectra show two notable absorption bands Figure 4. The first corresponds to the $\pi \rightarrow \pi^*$ transitions of pyridines, the second is due to metal-ligand charge transfer (MLCT) at longer wavelengths Table1.

CNTPAFe^{II}Cl$_2$ λ, nm, (ε, mmole^{-1}.cm^{-2})	**$(CN)_2$TPAFe^{II}Cl$_2$** λ, nm, (ε, mmole^{-1}.cm^{-2})	**$(CN)_3$TPAFe^{II}Cl$_2$** λ, nm, (ε, mmole^{-1}.cm^{-2})
258 (9743)	***262 (10811)***	269 (12046)
389 (1963)	471 **(**1127)	451 (759)

Table1: UV-visible data of the CNTPAFeCl$_2$, (CN)2TPAFeCl$_2$ and (CN)3TPAFeCl$_2$ complexes and their molar extinction coefficients.

The charge transfer bands are wide and protrude into the visible region. Thus the (CN)2TPAFeCl$_2$ and (CN)3TPAFeCl$_2$ complexes absorb in the blue-green, which gives the complexes a reddish color **Figure 4**. This phenomenon is less marked for CNTPAFeCl$_2$ which appears red-orange since it absorbs more in the blue-violet. The UV-visible data of the CNTPAFeCl$_2$, (CN)2TPAFeCl$_2$ and (CN)3TPAFeCl$_2$ complexes and the values of the molar extinctions coefficients are listed in Table 1.

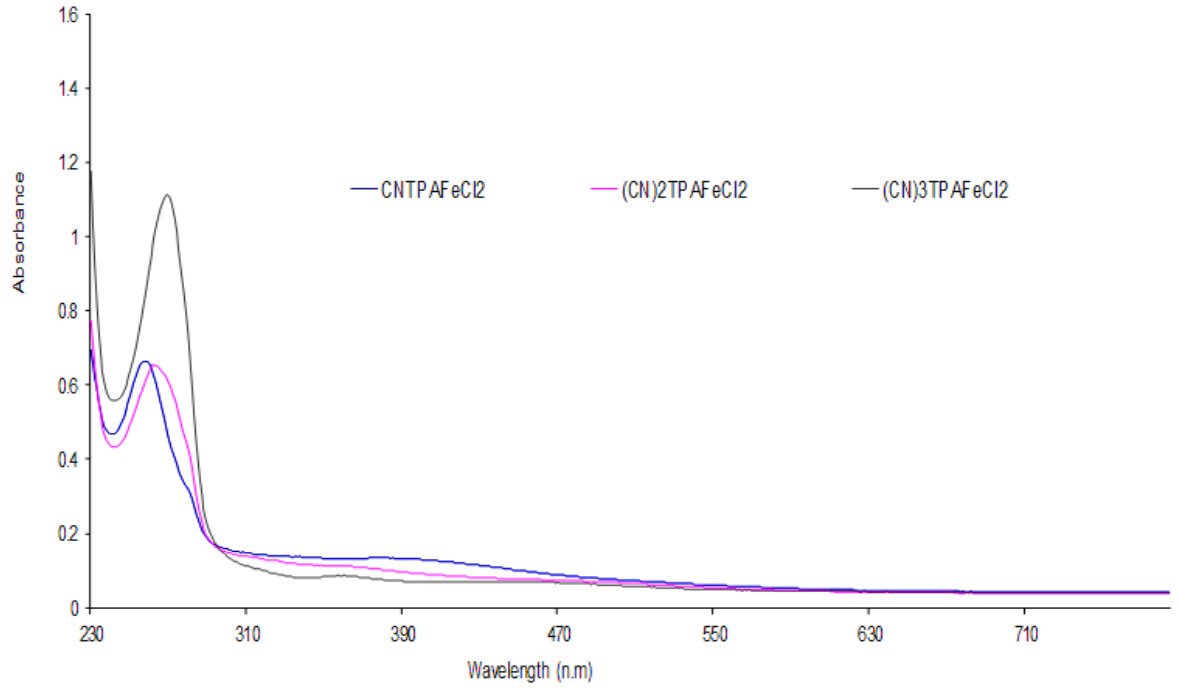

Figure 4 : UV-visible spectra of the CNTPAFeCl2, (CN)2TPAFeCl2, and (CN)3TPAFeCl2 complexes..

II-Paramagnetic 1H NMR in CD3CN:

Not widely used in molecular chemistry, this technique is applicable to certain paramagnetic derivatives. Under the influence of a paramagnetic ion present within the molecule, in our case iron, the resonances of the nuclei studied widen and are displaced (-50 <ppm <200). Iron is at oxidation state (+II), so the metal has a 3d6 configuration. In our case, the appearance of signals in the paramagnetic region allows us to state that the iron is in a strong spin state, S = 2, Figure 5.

Furthermore, the signals observed can be classified into two groups: a) those which are very large, here the α and

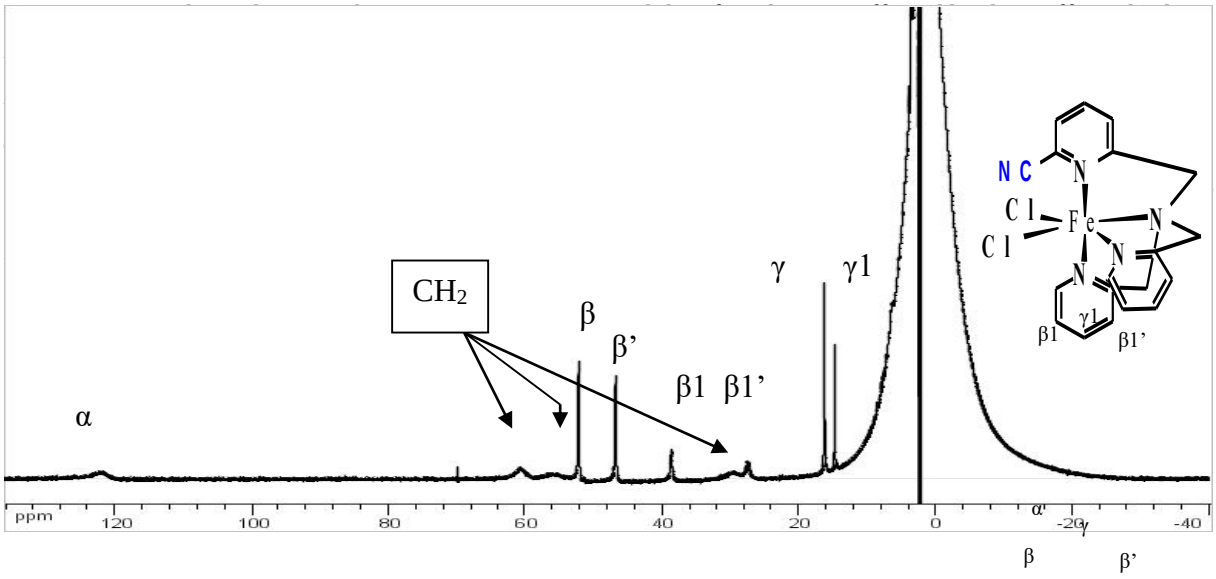

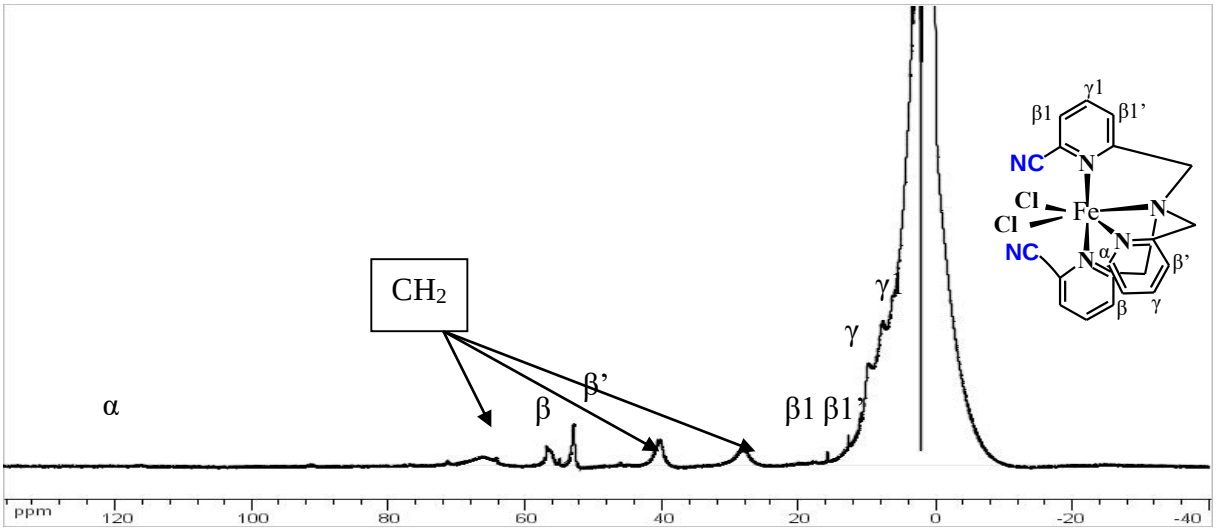

Figure 5: Paramagnetic 1H NMR spectrum for the CNTPAFeCl2 and (CN) 2TPAFeCl2 complexes.

A priori, in both cases, the widths at mid-height correspond to the presence of a pseudo-octahedral species: the spectrum of CNTPAFeCl2 is very close to that measured in BrTPAFeCl2. The lines of CNTPAFeCl2 are noticeably wider, but still in a range of width at half height corresponding to a pseudo-octahedral geometry.

The case of the(CN)3TPAFeCl2 complex is separate: a priori, a low molecular extinction coefficient observed in UV-visible solution for the MLCT transition suggests a bipyramid geometry with a trigonal base for the metal in this complex (Figure 6). We would therefore expect a broad line spectrum, very poorly defined, close to that described with Br3TPAFeCl2 [13].

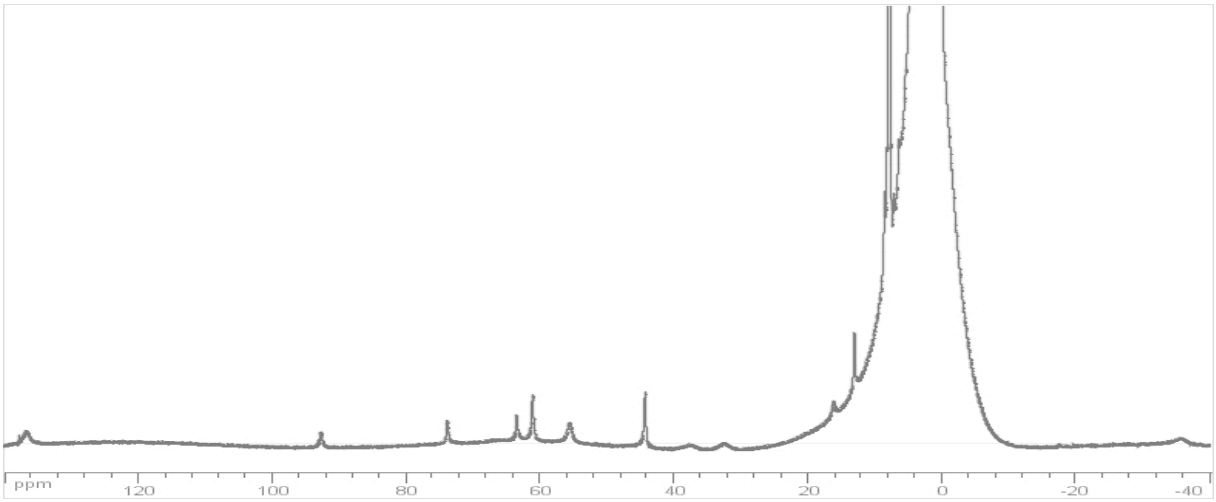

Figure 6 : Paramagnetic 1H NMR spectrum obtained after dissolution in CD3CN of the (CN)3TPAFeCl2 complex.

In reality, the spectrum, reproduced in the figure above shows the presence of fine lines next to larger signals. Obtaining this spectrum is reproducible, and it has been verified that the air-free conditions have been observed. We will see in the discussion section that this spectrum probably does not correspond to the species studied by UV-visible and conductimetry, the deuterated solvent containing a significant amount of water (including deuterated water) capable of reacting.

III. Conductimetry measurements:

The molar conductimetry measurements are carried out in solution in acetonitrile, at room temperature and at a given concentration **Table 2**. They make it possible to know the nature of the solute, charged or neutral species. Here are the values obtained for a concentration of around 0.001 M:

	$TPAFeCl_2$	**$CNTPAFeCl_2$**	**$(CN)_2TPAFeCl_2$**	**$(CN)_3TPAFeCl_2$**
$\Lambda(S.mol^{-1}.cm^2)$	30.34	13.80	21.03	25.15

Table 2: Molar conductimetry measurements show that the complexes in solution remain neutral

In view of the values presented in the table above and the values previously found in the chemistry of dichloroferrous complexes, it is highly probable that the complexes in solution remain neutral. The mono and bi charged complexes all have a molar conductivity equal to or greater than 100 $S.mol^{-1}.cm^{-2}$.

Structural characterization by X-ray diffraction.

The technique used to obtain single crystals is that of diffusion of diethyl ether in an acetonitrile solution of the complexes, free from oxygen in sealed glass tubes.

We made crystallization tubes for our three complexes with acetonitrile as solvent, and diisopropyl ether as a counter solvent, all of which was carried out under an oxygen-free atmosphere.We were able to obtain single crystals for the $CNTPAFeCl_2$ and

$(CN)2TPAFeCl_2$ complexes. The structures are shown below.

$CNTPAFeCl_2$

This complex crystallizes in a monoclinic system, in the space group P21 / n. The parameters of the mesh are a = 8.5600 (5) Å, b = 15.5940 (9) Å, c = 14.7230 (11) Å with angles α = 90 °, β = 103.271 (2) °, γ = 90 °. The number of patterns per stitch is Z = 4. A Mercury digraph is shown in Figure 7.

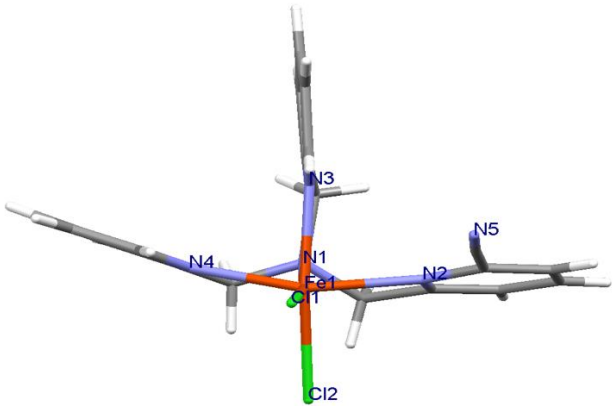

Figure 7: Mercury representation of the $CNTPAFeCl_2$ complex. The main distances and angles are given in

Table 3.

(CN)2TPAFeCl$_2$.

This complex crystallizes in a monoclinic system, in the space group P21 / n. The parameters of the mesh are a = 12.465 (4) Å, b = 14.212 (5) Å, c = 13.312 (5) Å with angles α = 90 °, β = 102 °, γ = 90 °. The number of patterns per stitch is Z = 4. A Mercury diagram is shown in Figure 8.

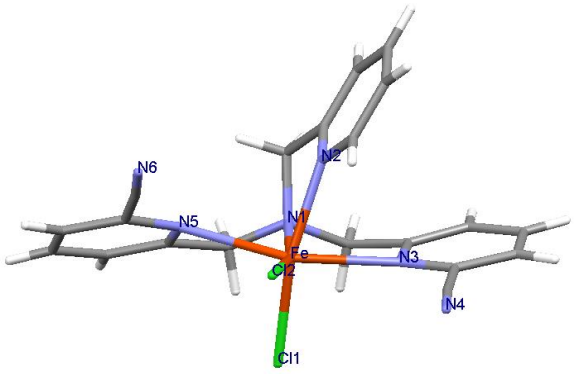

Figure 8: Mercury representation of the (CN)2TPAFeCl$_2$ complex.

The main distances and angles are given in Table 3.

(CN)$_2$TPAFeCl$_2$		CNTPAFeCl$_2$	
Les distances	Les angles	Les distances	Les angles
Fe N2 2.189(3)Å Fe N1 2.234(2)Å Fe Cl2 2.3217(8)Å Fe N3 2.325(3)Å Fe Cl1 2.3976(10)Å Fe N5 2.414(3)Å	N2 Fe N1 77.59(9)° N2 Fe Cl2 95.33(7)° N1 Fe Cl2 165.28(7)° N2 Fe N3 77.95(10)° N1 Fe N3 76.21(9)° Cl2 Fe N3 115.30(7)° N2 Fe Cl1 163.76(7)° N1 Fe Cl1 90.89(7)° Cl2 Fe Cl1 98.35(3)° N3 Fe Cl1 88.28(7)° N2 Fe N5 92.14(10)° N1 Fe N5 70.39(9)° Cl2 Fe N5 97.30(6)° N3 Fe N5 146.49(9)° Cl1 Fe N5 94.75(7)° C12 N3 Fe 129.3(2)°	Fe1 N3 2.202(4)Å Fe1 N1 2.215(4)Å Fe1 N2 2.266(4)Å Fe1 N4 2.312(4)Å Fe1 Cl1 2.3496(15)Å Fe1 Cl2 2.4324(15)Å	N3 Fe1 N1 81.26(15)° N3 Fe1 N2 77.34(16)° N1 Fe1 N2 75.53(16)° N3 Fe1 N4 83.02(15)° N1 Fe1 N4 146.20(17)° N2 Fe1 N4 71.92(16)° N3 Fe1 Cl1 97.20(12)° N1 Fe1 Cl1 96.98(13)° N2 Fe1 Cl1 171.22(12)° N4 Fe1 Cl1 114.58(12)° N3 Fe1 Cl2 166.97(12)° N1 Fe1 Cl2 100.32(12)° N2 Fe1 Cl2 90.46(11)° N4 Fe1 Cl2 88.88(11)° Cl1 Fe1 Cl2 95.45(5)°

Table 3: Interatomic distances and principal angles in CNTPAFeCl$_2$, (CN)2TPAFeCl$_2$ complexes.

Common points between these two structures:

In both cases, the metal is in a very distorted octahedral environment, as evidenced by the N-Fe-N angles between 70 and 80 °. These values are not surprising when you consider that these angles are part of a five-membered (pentagon) ring. We are dealing here with a Fe (II) complex. In addition, by analyzing the distances

between iron and nitrogen, we see that they are all greater than 2 Å, which is characteristic of a strong spin complex (weak field). If we look at the molecule in the equatorial plane, on the chlorine side, we see that the nitrile function (s) point outwards, which probably reflects the effects of electronic repulsion between the nitriles and the chlorines. For the di ***nitrile*** ligand derivative, the strain is very large and the nitriles point in opposite directions.

Trans-equatorial deformation:

We defined in Chapter 4 the parameter ρ called "trans-equatorial deformation", as the product of the dihedral angle ϕ and the torsion angle θ of the two axial pyridines. If we compare the structures of the $TPAFeCl_2$, $CNTPAFeCl_2$ and $(CN)2TPAFeCl_2$ complexes, we realize that the transequatorial deformation becomes very important in the case of the latter complex. Table 4 lists the measured values

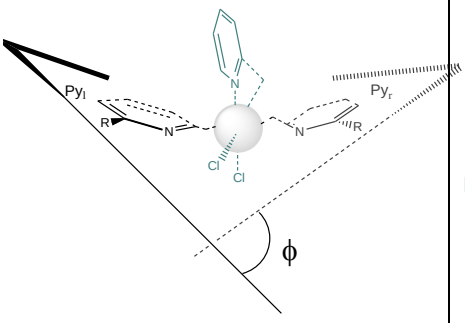

ϕ : the angle of the dihedron Py_l – Py_r

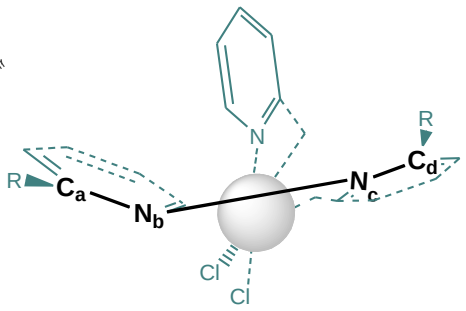

θ: torsion angle Ca-Nb-Nc-Cd

	ϕ, °	**θ, °**	**ρ, °²**
$TPAFeCl_2$	6.75	3.08	20.8
$CNTPAFeCl_2$	26.19	1.78	46.6
$(CN)2TPAFeCl_2$	33.90	6.28	212.9

Table 4: Measured values of ϕ, dihedral angle between two pyridines in trans, of θ: angle of torsion between two pyridines in trans, and ρ = ϕ x θ :trans angular deformation parameter in pseudo-octahedral complexes.

Deformation of nitriles:Structural analysis shows that the C_{arom}-CN segment is not linear. The two diagrams below show a top view of the equatorial plane of the complexes.

In $CNTPAFeCl_2$, the corresponding angle is 173.8 °, significantly different from the expected 180 °. In fact, it is also noted that this nitrile is in contact with the equatorial coordinated chlorides, since the corresponding distances are 3.70 and 3.69 Å.

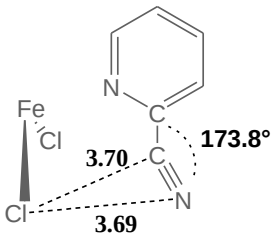

Nitrile does not interact much with the axial chloride ion, since the distances are greater than 5 Å. The same effect is observed with (CN)2TPAFeCl$_2$:

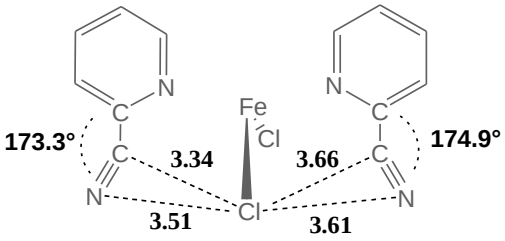

It is therefore very possible that the trans-equatorial deformations, visualized below, reflect a marked steric gene.

3. Reactivity with respect to dioxygen of the *nitrile* series complexes:

We mentioned in the previous chapters that in the absence of reactive substituents on the ligand, the oxygenation reaction led directly to the formation of diferric binuclear complexes with µ-oxo bridges. We showed in Chapter 4 that with identical geometry, the complexes react more quickly as the metal is depleted in electrons. A priori, in view of the very electro-deficient nature of the ***nitrile*** ligands, the corresponding complexes should be among the most reactive. We will now validate or not this idea.

I. Suivi par spectroscopie UV-visible.

The bubbling of dry oxygen into a complex solution results in a very gradual color change in the three complexes CNTPAFeCl$_2$, (CN)2TPAFeCl$_2$, (CN)3TPAFeCl$_2$. This change takes a few minutes with (CN)2TPAFeCl$_2$ and (CN)3TPAFeCl$_2$; in the case of CNTPAFeCl$_2$, the medium turns slightly brown to become distinctly brown after a few hours.

	CNTPAFeCl$_2$	**(CN)$_2$TPAFeCl$_2$**	**(CN)$_3$TPAFeCl$_2$**
Color change	Red-brown 15 hours	Red-brown 30 minutes	Chestnut 15 minutes

The kinetics can be easily followed by UV-visible spectroscopy. This technique also makes it possible to determine whether there is only a single spectroscopic step, or whether intermediates can be detected.

Figure 9: a), b) and c) reports the spectroscopic changes observed for CNTPAFeCl$_2$, (CN)2TPAFeCl$_2$, and (CN) 3TPAFeCl$_2$, respectively. It is easy to see that the oxygenation reaction of CNTPAFeCl$_2$ is slow and gradual. The spectrum no longer changes after about 15 hours, and the absorptions observed at λ = 327 nm and λ = 380 nm are characteristic of the presence of a diferric µ-oxo species of symmetrical structure as the end product of the reaction.

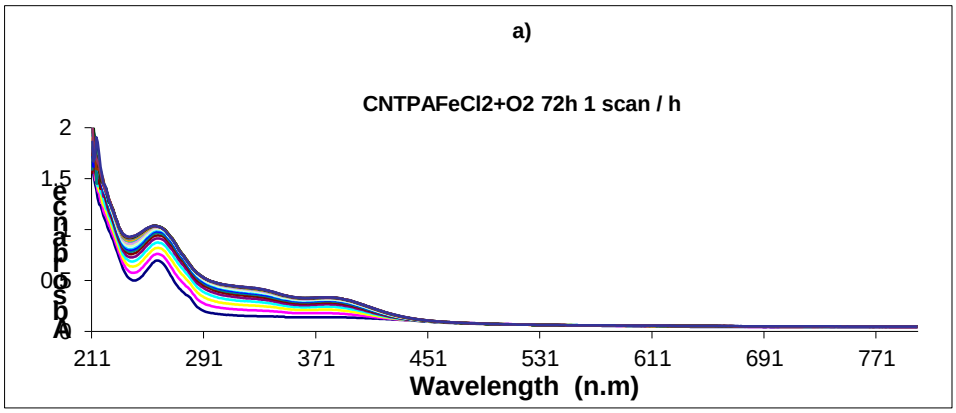
a)
CNTPAFeCl2+O2 72h 1 scan / h
Absorbance
2
1.5
0.5
0
211
291
371
451
531
611
691
771
Wavelength (n.m)

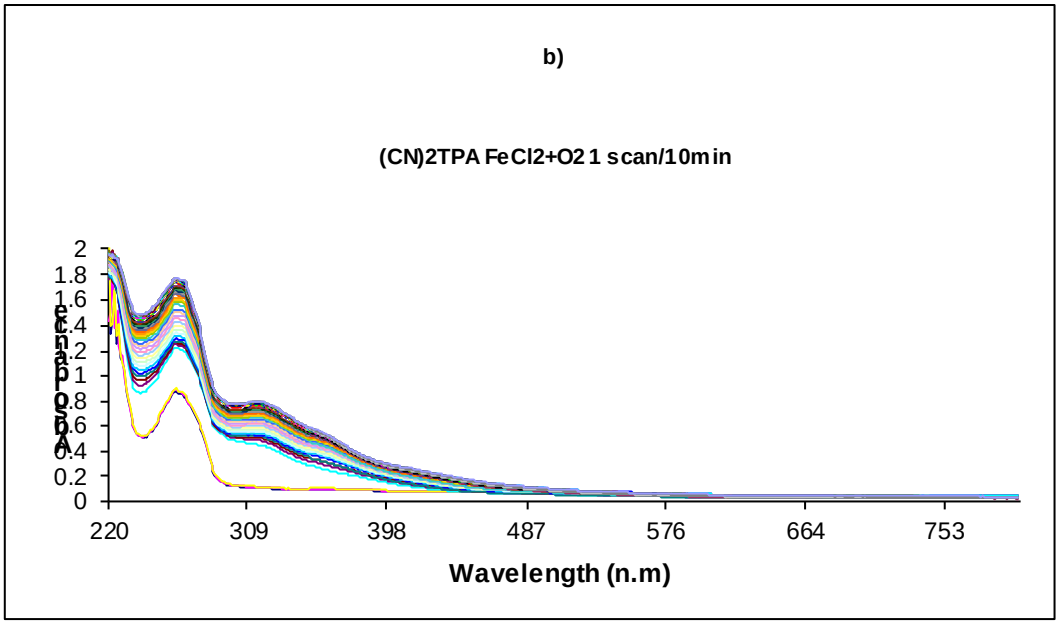
b)
(CN)2TPA FeCl2+O2 1 scan/10min
Absorbance
2
1.8
1.6
1.4
1.2
1
0.8
0.6
0.4
0.2
0
220
309
398
487
576
664
753
Wavelength (n.m)

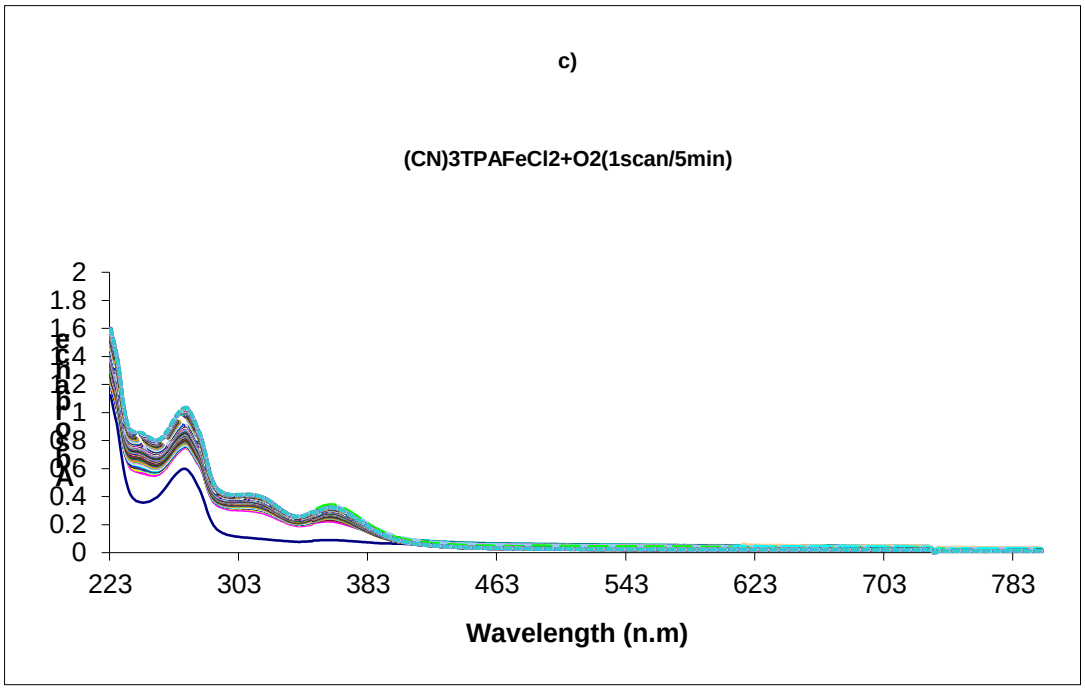

Figure 9: UV-vis tracking of the oxygenation reaction of the complexes: a) CNTPAFeCl$_2$, b) (CN)2TPAFeCl$_2$, c) (CN)3TPAFeCl$_2$.

The oxygenation of (CN)2TPAFeCl$_2$ appears to take place in two stages: one starts instantly, and stabilizes in about 30 minutes, a rather ill-defined spectrum is obtained. The second step is more gradual, and the observation of two absorptions at λ = 316 nm and λ = 358 nm suggests the presence of a μ-oxo diferric species. The general shape of the spectrum suggests a different structure of the μ-oxo segment, intermediate between a symmetrical complex and an asymmetric species. The reaction is considered to be complete after 4 hours.

Finally, (CN)3TPAFeCl$_2$ is the most rapidly reacting complex, and its oxygenation also appears to occur in two stages. As with the (CN)2TPAFeCl$_2$ complex, the first step starts instantly and stabilizes in 15 minutes. The second step is more progressive, we observe two absorption bands at λ = 315 nm and λ = 255 nm which suggest the presence of a diferric μ-oxo species of symmetrical structure. The reaction is considered complete after 90 minutes.

II. Paramagnetic 1H NMR monitoring of the CNTPAFeCl$_2$ oxygenation reaction:

1H NMR in CD3CN: the spectra obtained for the complexes in the absence of dioxygen have a strong paramagnetic character, the signals appearing between –50 and 160 ppm. During the oxygenation reaction, we form a binuclear complex linked by a μ-oxo bridge. The presence of a μ-oxo bridge strongly changes the spectrum. Indeed, an antiferromagnetic coupling phenomenon is observed between the two metals, which allows the complex to acquire a pseudo diamagnetic character.

The main effect of oxygenation of the CNTPAFeCl$_2$ complex is to suppress the signals of the complex. After 4 hours, the presence of free ligand is detected. After 24 hours, there is still a little starting material, but most of the signals are grouped together in the form of broad peaks located between 20 and –10 ppm (spectrum at t = 30min,

t = 3h, t = 24h , t = 72h, Figur10).

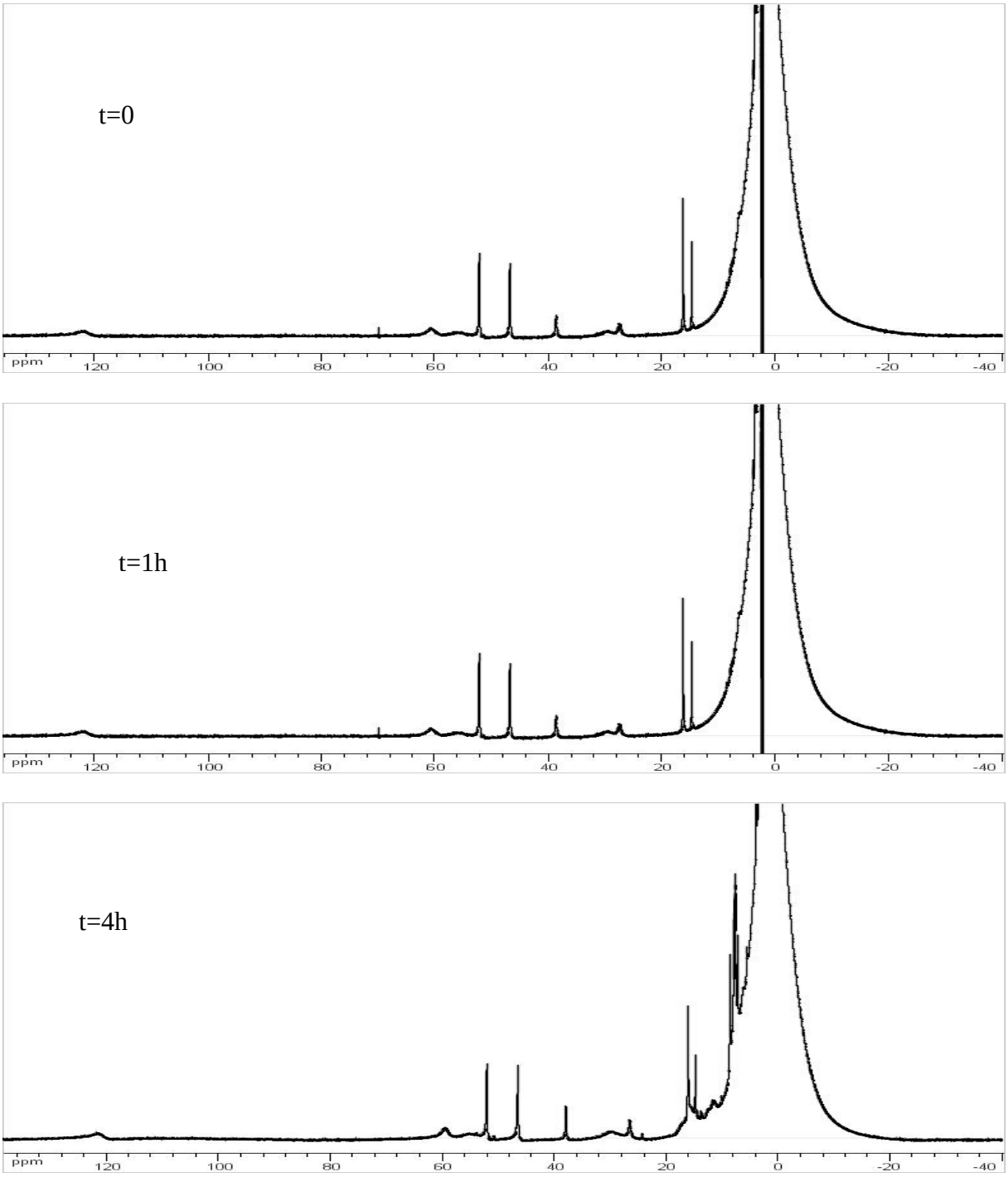

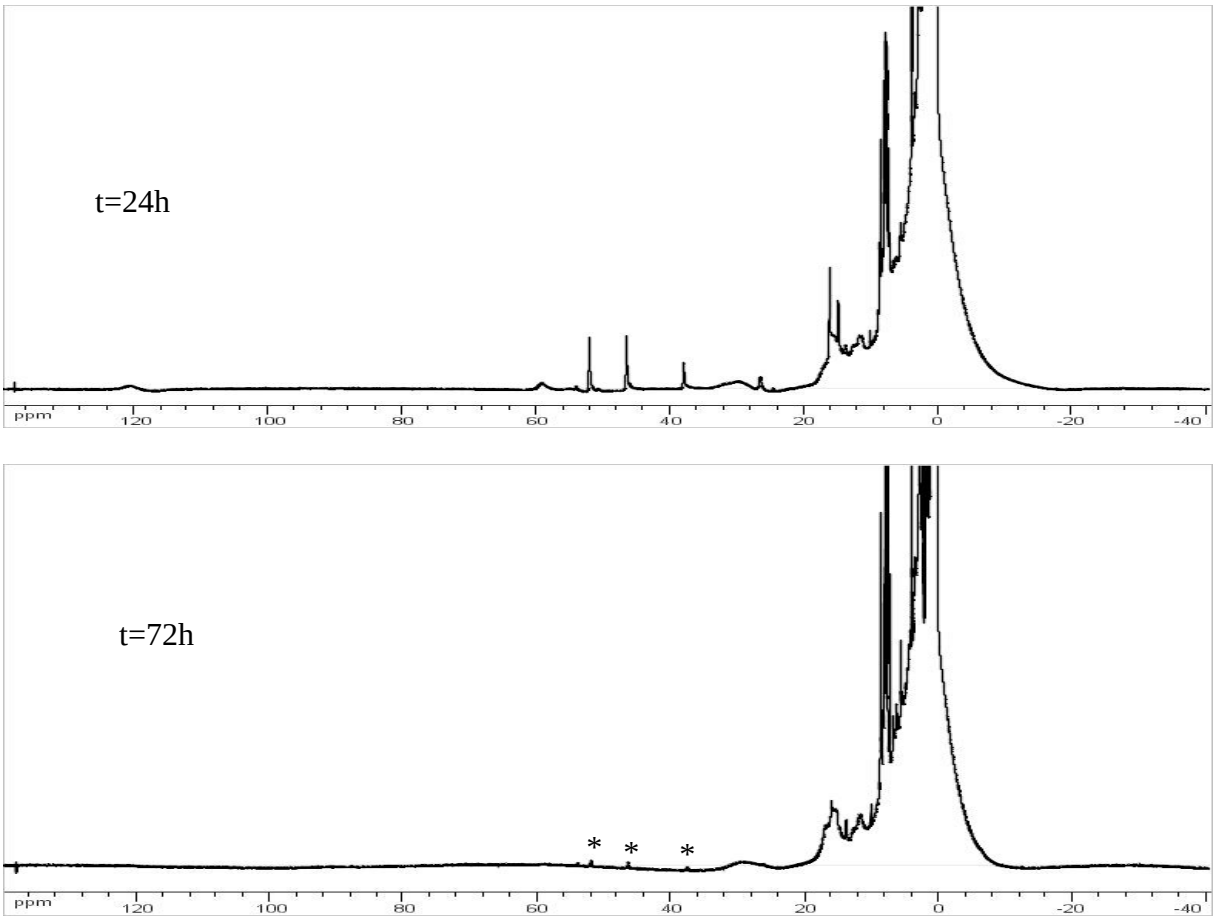

Figure 10: The 1H NMR spectra, for the oxygenation kinetics of the CNTPAFeCl$_2$ complex at: a) t = 0, b) t = 1h, c) t = 4h, d) t = 24h, e) t = 72h. The stars correspond to the signals of the traces of the starting product.

2) Reactivity in the presence of substrate.

The oxygenation mechanism of the complexes, Figure 11, shows that at some point an intermediate Fe $^{(IV)}$ - oxo species is formed. This species is very oxidizing, during the reaction in the absence of substrate, it reacts with a complex molecule to form a μ-oxo diferric species.

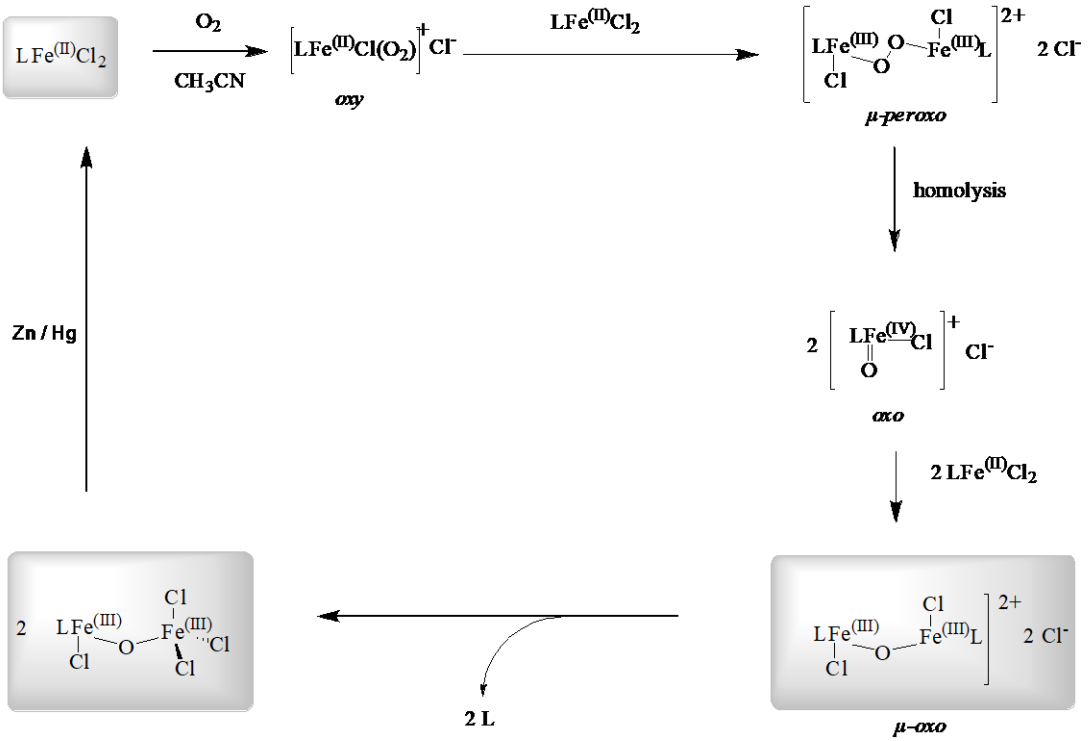

Figure 11:The oxygenation mechanism of the complexes.

It would therefore be conceivable that such a species in the presence of a substrate, such as cyclohexane, is capable of transferring oxygen to lead to the formation of an oxidized substrate. It is with this hope that we carried out the following experiments. The oxidation of cyclohexane to cyclohexanone has already been studied with complexes substituted by fluorine and we will compare the results with complexes substituted by nitrile groups. It is therefore a matter of reacting the three complexes with cyclohexane in the presence of O_2. We used zinc amalgam as the Fe $^{(III)}$ / Fe $^{(II)}$ reducing agent to regenerate reactive species during the reaction. In a schlenck tube, prepare a solution of known concentration of complex dissolved in acetonitrile, add cyclohexane, a few drops of zinc amalgam, and bubble oxygen. After one to two hours, a grayish solution is obtained, the acetophenone is added in a known quantity and the whole is filtered through Celite. Acetophenone is used as a reference for the analysis of GC gas chromatography results

.

Results: the first signal appears at 4.1 minutes and corresponds to the acetonitrile peak, which is the most intense. Then a few seconds later follows the cyclohexane signal, a low intensity peak. At around 6.6 minutes, the appearance of cyclohexanone is observed, a very weak peak and at the end of 11.6 minutes the reference signal, acetophenone, appears. The relationship below makes it possible to calculate the concentration of cyclohexanone and therefore the TON turn over number:

[cyclohexanone] = 1.2 [acetophenone] * Aire (cyclohexanone) / Aire (acetophenone)

TON = [cyclohexanone] / [catalyst]

Below are listed the results obtained:

	$TPAFeCl_2$	$TPACNFeCl_2$	$TPACN2FeCl_2$	$TPACN3FeCl_2$
TON	=8	=25	=84	=9

www.jst.org.in *DOI: https://doi.org/10.46243/jst.2022.v7.i02.pp54-76*

Conclusion

A series of TPA ligand substituted by 1, 2 and 3 nitrile groups was synthesized, characterized and complexed with $FeCl_2$. To date, these are the most electro-deficient ligands synthesized in the laboratory. The desire to create such a ligand is not trivial, in fact we are trying to demonstrate that the more electron-deficient the ligand, the more the metal center of the complex has a strong Lewis acid character (for a given geometry). This will increase the speed of O_2 coordination on the complex.

Three complexes were then prepared and characterized by different spectroscopic techniques, thus making it possible to predict their geometry in solution and in the solid state for (CN)2TPA$FeCl_2$ in particular. The compound (CN)2TPA$FeCl_2$ exhibits a strong deformation of the substituted pyridines relative to each other. Oxygenation is rapid for the bi- and tri-substituted complex, which confirms our hypothesis and probably leads to diferric μ-oxo species symmetrical for CNTPA$FeCl_2$ and (CN)3 TPA$FeCl_2$ and antisymmetric for (CN)2TPA$FeCl_2$.

We obtained the structures of the dichloroferrous complexes with the mono and bisubstituted ligands. It is obviously important to ensure that crystallization is carried out under anhydrous conditions. In these two complexes, the metal is found in a distorted octahedral geometry. The relative positions of pyridines, especially the angles of torsion of one to the other are important. For (CN)2TPA$FeCl_2$, the value of the trans-equatorial strain parameter is the highest listed in our laboratory. This is probably due to steric interactions between the nitrile substituents and the coordinated chloride ions.

The neutral electrolytic behavior of the complexes in solution, the general appearance of the 1H NMR spectra as well as the differences in the values of molecular extinction coefficients, suggest that the geometry as described in the solid state is maintained in solution.

We were unable to obtain single crystals of the (CN)3TPA$FeCl_2$ complex. The intensity of MLCT UV-visible absorption strongly suggests a trident mode of coordination for the ligand, similar to that described with F3TPA [3]. This would not be surprising given the significant deformations already observed with the disubstituted ligand: the increase in the steric gene would result in the decoordination of an aminomethyl pyridine arm.

The behavior of this complex in CD_3CN is quite peculiar: we expected a simple spectrum with broad lines. Rather fine lines are obtained, and the spectrum is quite complex.

We show, in mono and bisubstituted series, that the hydrolysis of the nitrile functions by water added to the ferrous complexes is very real. We believe this is related to the proximity of a nitrile function and a water molecule both activated by the presence of an electron-deficient metal center. We hypothesize that this deficiency, which is major in the case of a trisubstituted complex, would be the basis of a strong reactivity of the metal center for the residual water of the deuterated solvent, which has not been dried. In general, neutral complexes of single ligands are yellow in color.

The compounds we have synthesized all show a reddish color. If we take a closer look at the absorption spectra, we see that the bands due to charge transfer are either very wide ($CNTPAFeCl_2$), or clearly shifted towards the red [$(CN)2TPAFeCl_2$ and $(CN)3TPAFeCl_2$] by compared to the already known complexes (370 nm < λ <430nm for halogenated, methyl or substituted aryl ligands [2,3]). We don't know the reason. Is this due to the effect of the nitrile substituents, which are very attractive, or to the deformation of the cyanated pyridines? A theoretical study would no doubt provide some answers to these questions.

A word about the behavior of complexes in electrochemistry: we are looking to obtain complexes whose metallic center is deficient in electrons. A priori the comparison, within a series, of the Fe (III) / Fe (II) redox potentials could provide an indication as to the Lewis acidity of the metal center. This is not easy, the complexes having a tendency, from the disubstitution of the ligand, to dissociate in a strong electrolytic medium. Some preliminary tests failed to obtain well-defined redox waves for the entire series of ***nitrile*** tripod complexes. This had already been observed for the fluorinated series. We will simply say that with the same geometry, it seems logical that the electron deficiency of the metal center increases with the substitution of the ligand by electron withdrawing groups.

Referances:

(1) Bioinorganic Chemistry : A short course. Roat-Malone, R.M., Wiley Interscience. **2002**

(2) Solomon, E. I., Brunold, T. C., Davis, M. I., Kemsley, J. N., Lee, S. K., Lehnert, N., Neese, F., Skulan, A. J., Yang, Y. S., Zhou, J., *Chem. Rev*., **2000**, *100*, 235-349.

(3) Coordination Chemistry Reviews 200-202, **2000,** 443-485

(4) Kryatov, S.V., Rybak-Akimova, E.V., MmacMurdo, V.L., Que, L.Jr., *Inorg Chem* **2001**, 40, 2220-2228 and many references herein

(5)-Michael P .Jensen ,Steven J.Lange, Mark, Emily L.que And Lawrence Que , Jr. JACS ,**2003**, *125, 2113*-2128.

(6) Lehnert, N., Ho, R.Y.N., Que, L.Jr., Solomon, E.I., *J. Am Chem Soc.*, **2001**, 123, 8271-8290.

(7) Costas, M., Tipton A.K., Chen, K., Jo, D.H., Que, L.Jr, *J. Am Chem Soc.*, **2001**, 123, 6722-6723.

(8) Jo, D.H., Chiou, Y.M., Que, L.Jr., *J.Am.Chem.Soc*., **2001**, 40, 3181-3190.

(9) Chiou, Y.M., Que, L.Jr., *J.Am.Chem.Soc*., **1995**, 117, 3999-4013.

(10) Zang, Y., Que, L.,Jr., *Inorg Chem* **1995**, 34, 1030-1035.
(11) ZS Malek, D Sage, P Pévet, S Raison Endocrinology 148 (11), 5165-5172.

(12) ZS Malek, H Dardente, P Pevet, S Raison European Journal of Neuroscience 22 (4), 895-901.

(13) ZS Malek, P Pevet, S Raison Neuroscience 125 (3), 749-758.

(14) ZS Malek, LM Labban International Journal of Neuroscience, 1-7.

(15) ZS Malek, L Labban European Journal of Pharmaceutical and Medical Research 6 (11), 527-532.

(16) Z Malek Journal of AlBaath University 40 (4), 39-62

(17) ZS Malek Tishreen University Journal for Research and Scientific Studies 40, 2018.

(18)-Mandon, D., Machkour, A., Goetz, S., Welter, R., Inorg. Chem 2002., Vol.41,No.21,

(19)- Machkour, A., Mandaon, D., Welter, R., Inorg. Chem. 2004, 43, 4, 1545–1550

(20)- Kappock, T. J; Caradonna, J. P.; Chem.Rev. 1996, 96, 2659-2756.

(21)- Solomon, E. I.; Brunold, T. C.; Mindy I. D.; Kemsley, J. N.; Sang-Kyu Lee.; Lehnert, N.; Neese, F.; Skulan, A. J.; Yi-Shan Y.; and Jing Z.; Chem.Rev. 2000, 100, 235-349.

(22)- Goodwill, K. E.; Sabatier, C.; and Stevens, R. C.; Biochemistry 1998, 37, 13437-13445.

(23)- Wang Lin.; Erlandsen, H.; Haavik, J.; Knappskog, P. M.; and Stevens R. C , Biochemistry 2002, 41, 12569-12574.

(24)- Nordlund P.; in Handbook of Metalloproteins (Eds.: I. Bertini,A. Sigel, H. Sigel), Marcel Dekker, New York, 2001, pp. 461 -570.

(25)- Xia, T.; Gray, D. W. ; Shiman, R. J.; Biol. Chem. 1994, 269, 24657-24665.

(26)- Francisco W. A.; Tian G.; Fitzpatrick P. F.; and Klinman J. P , J. Am. Chem. Soc.;1998, 120, 4057 –4062.

(27)Arianna B.; Margareta R.A.; Per E.M .S.; Chem. Eur. J. 2003, 9,106-115

(28)- Flatmark T.; Stevens R. C.; Chem. Rev. 1999, 99, 2137-2160

(29)- Kemsley, J. N. ; Mitic, N.; Loeb-Zaleski, K.; Cradonna, J. P.; Solomon, E. I.; J. Am. Chem. Soc. 1999, 121, 1528-1536.

(30)- Dix, T. A.; Kuhn, D. M.; Benkovic, S. J.; Biochemistry 1987, 26, 3353-3361.

(40)- Hillas, P. J.; Fitzpatrick, P. F.; Biochemistry 1996, 35, 6969-6975.

(41)- Dix, T. A.; Bollag, G. E.; Domanico, P. L.; Benkovic, S. J.; Biochemistry 1985, 24, 2955-2958.

(42)- Gardner, H. W.; Biochim. Biophys. Acta 1991, 1084, 221-239.

(43)- Thallaj, N., Machkour, A., Mandon, D., Welter, R., New. J. Chem., 2005, 29, 1555 – 1558

(44)- Machkour, A., Mandon, D., Lachkar, M., Welter, R., Inorg. Chim. Acta, 2005, 358, 839 – 843.

(45)- Bioinorganic Chemistry : A short course. Roat-Malone, R.M., Wiley Interscience. 2002.

(46)- Solomon, E. I., Brunold, T. C., Davis, M. I., Kemsley, J. N., Lee, S. K., Lehnert, N., Neese, F., Skulan, A. J., Yang, Y. S., Zhou, J., Chem. Rev., 2000, 100, 235-349.

(47)- Coordination Chemistry Reviews 200-202, 2000, 443-485

(48)- Kryatov, S.V., Rybak-Akimova, E.V., MmacMurdo, V.L., Que, L.Jr., Inorg Chem 2001, 40, 2220-2228 and many references herein.

(49)- Michael P .Jensen ,Steven J.Lange, Mark, Emily L.que And Lawrence Que , Jr. JACS ,2003, 125, 2113-2128.

(50)- Lehnert, N., Ho, R.Y.N., Que, L.Jr., Solomon, E.I., J. Am Chem Soc., 2001, 123, 8271-8290.

(51)- Costas, M., Tipton A.K., Chen, K., Jo, D.H., Que, L.Jr, J. Am Chem Soc., 2001, 123, 6722-6723.

(52)- Jo, D.H., Chiou, Y.M., Que, L.Jr., J.Am.Chem.Soc., 2001, 40, 3181-3190.

(53)- Chiou, Y.M., Que, L.Jr., J.Am.Chem.Soc., 1995, 117, 3999-4013.

(54)-bZang, Y., Que, L.,Jr., Inorg Chem 1995, 34, 1030-1035.

(55)- Thallaj, N. K. Damascus University Journal for Basic Sciences. 34 (1) 2018.

(56)- Thallaj. N. K. Journal of AlBaath University (39) 2017.

(57)- Thallaj. N. K. Tishreen University Journal for Research and Scientific Studies 38 (6) 2016.

(58)- N. K. Thallaj, P.Y. Orain, A. Thibon, M. Sandroni, R. Welter and D. Mandon, Inorg. Chem. 2014, 53 (15), 7824-7836.

(59)- A. Wane, N. K. Thallaj, and D. Mandon Chem. Eur. J. 2009, 15, 10593 -10602.

(60)- N. K. Thallaj, O. Rotthaus, L. Benhamou, N. Humbert, M. Elhabiri, M. Lachkar, R. Welter, A.M. Albrecht-Gary, and D. Mandon, Chem. Eur. J. 2008, 14(22) 6742-6753.

(61)- N. K. Thallaj, J. Przybilla, R. Welter and D. Mandon, J. Am. Chem. Soc. 2008, 130, 2414-2415.

(62)- N. K. Thallaj, D. Mandon and K. A. White, Eur. J. of Inorg. Chem., 2007, 44–47.

(63)- Machkour, N. K. Thallaj, L. Benhamou, M. Lachkar and D. Mandon, Chem. Eur. J., 2006, 12, 6660 – 6668.

(64)- N. K. Thallaj, A. Machkour, D. Mandon and R. Welter, New J. Chem., 2005, 29, 1555–1558.

(65)- Thallaj, N.; International journal of applied chemistry and biological sciences 2021, 2 (4), 65-77.

(66)- Thallaj, N.; Indian Journal of Advanced Chemistry (IJAC)2021, 1 (2), 20-26.

(67)- Thallaj, N.; International Journal of Research Publication and Reviews (IJRPR),2021, 2 (10), 951-959.

(67)- V. Caprio, J. Mann, J. Chem. Soc., Perkin Trans. 1, 1998, 3151–3155.

(68)- Da Mota, M. M.; Rodgers, J.; Nelson, S. M.; J. Chem. Soc. (A). 1969, 2036-2044.

(69)- Andris, E.; Navrátil, R.; Jasik, J.; Puri, M.; Costas, M.; Que, L., Jr.; Roithová, J. J. Am. Chem. Soc. 2018, 140, 14391-14400

(70)- Cutsail III, G.; Banerjee, R.; Zhou, A.; Que, L., Jr.; Lipscomb, J. D.; DeBeer, S. J. Am. Chem. Soc. 2018, 140, 16807–16820.

(71)- Fan, R.; Serrano-Plana, J.; Oloo, W. N.; Draksharapu, A.; Delgado-Pinar, E.; Company, A.; Martin-Diaconescu, V.; Borrell, M.; Lloret-Fillol, J.; García-España, E.; Guo, Y.; Bominaar, E. L.; Que, L., Jr.; Costas,
(72)- M.; Münck, E. J. Am. Chem. Soc. 2018, 140, 3916-3928.